Journal of Thermal Analysis and Calorimetry, Vol. 74 (2003) 923–930

THERMOANALYTICAL STUDY ABOUT HISTIDINE AND CYSTEINE–CADMIUM INTERACTIONS

R. F. de Farias [1], *L. M. Nunes* [2] *and C. Airoldi* [2*]

[1]Departamento de Química, Universidade Federal de Roraima, 69310-270 Boa Vista, Roraima, Brasil
[2]Instituto de Química, Universidade Estadual de Campinas, Caixa Postal 6154, 13084-971 Campinas, São Paulo, Brasil

(Received December 13, 2002 in revised form; July 22, 2003)

Abstract

Infrared spectroscopy, thermogravimetry and differential scanning calorimetry techniques were used to study the metal–amino acid interactions for adducts of the general formula $CdCl_2 \cdot nL$ (n=1.0 or 1.5 and L=histidine or cysteine). After characterization the thermal degradation process was kinetically followed by a non-isothermal method. The infrared data confirmed that the cation is coordinated the carboxylic oxygen atoms of the amino acid molecules. The thermogravimetric results indicated that the main step of the thermal degradation of all amino acid adducts is connected to the rupture of the metal–ligand bonds, to give the associated activation energies values of 77, 44, 55 and 41 kJ mol^{-1} for $CdCl_2 \cdot nL$, n=1.0 and 1.5, for histidine and cysteine, respectively.

Keywords: cadmium, cysteine, histidine, thermogravimetry

Introduction

Amino acids compose the building blocks of proteins that are chemical species indispensable to perform a huge of biological functions [1]. The basic atoms disposed on the main chains of these molecules are available to coordinate cations and the investigations on metal–amino acid interactions can be used to understand, for example, the poisoning role of some elements in living organisms [2]. The great majority of enzymes have the active site formed by metal–binding moieties [2], in which histidil and cysteinil groups can be involved [3]. On the other hand, the action of drug [3] can also be clarified through the knowledge of the metal–amino acid interactive process. A schematic representation of histidine and cysteine molecules is shown in Fig. 1.

Amino acids have also been extensively studied as components of inorganic–organic hybrid materials [4, 5], and many investigations dealing with the metal–amino acid interactions, involving a series of important metal like as copper [6], aluminum [7], platinum [8] and mercury [9] have been involved.

* Author for correspondence: E-mail: airoldi@iqm.unicamp.br

1388–6150/2003/ $ 20.00

Akadémiai Kiadó, Budapest
Kluwer Academic Publishers, Dordrecht

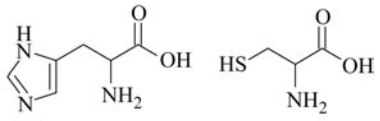

a b

Fig. 1 Structure of a – histidine and b – cysteine molecules

Thermogravimetry and differential scanning calorimetry (DSC) techniques were successfully employed not only to follow the thermal degradation of amino acids [10], but also to study metal–amino acid interaction [11]. Normally, in this kind of investigation, the kinetic parameters for the thermal degradation of the obtained adducts, were calculated by using a non-isothermal procedure [11]. The conclusions obtained by using thermogravimetry and differential scanning calorimetry are supported and completed by the solution calorimetry results [12].

The aim of this publication is to study, by using infrared, thermogravimetric, differential scanning calorimetry and non-isothermal kinetic thermogravimetric data, the cadmium–amino acid interactions, taking into account the adducts of the general formula $CdCl_2 \cdot n$L, were *L*=histidine (his) or cysteine (cys); *n*=1.0 or 1.5.

Experimental

The adducts of the general formula $CdCl_2 \cdot n$L, *n*=1.0 or 1.5 and *L*=his or cys, were prepared as previously described for cadmium–glycine compounds [11, 12], by dissolving stoichiometric amounts of cadmium chloride (Merck), histidine (Aldrich) or cysteine (Aldrich) in double distilled water. After mixing the desired solutions, the solvent was slowly evaporated during five days at room temperature. The synthesized adducts were dried under vacuum at room temperature for 8 h. The adducts of histidine were obtained as white crystals whereas the compounds of cysteine exhibited a pasty consistence.

Carbon, nitrogen and hydrogen contents were determined using a Perkin Elmer microelemental analyzer. The obtained results are in good agreement with the expected stoichiometries for the adducts, within an error of ±5%. The infrared spectra were recorded in a Bomem apparatus in the 4000–400 cm^{-1} range, with a resolution of 4 cm^{-1}. The spectra were obtained from powders in KBr discs for all the adducts. Thermogravimetric (TG) curves were obtained in a Shimadzu TGA 50 apparatus. The differential scanning calorimetric (DSC) curves were recorded in a DuPont 2000 apparatus. Both, TG and DSC curve were obtained in argon atmosphere with a heating rate of $8.3 \cdot 10^{-2}$°C s^{-1}. The non-isothermal thermogravimetric kinetic data were obtained by using the Coats–Redfern method [13].

Results and discussion

The elemental analysis results are summarized in Table 1 and are in agreement with the following expected formula $CdCl_2$·his, $CdCl_2$·1.5his, $CdCl_2$·cys and $CdCl_2$·1.5cys for the synthesized adducts.

Table 1 Experimental and (calculated) carbon, nitrogen and hydrogen percentages obtained from the elemental analysis for cadmium–histidine and cadmium–cysteine adducts

$CdCl_2$·*n*L	Carbon	Nitrogen	Hydrogen
$CdCl_2$·hys	22.4 (21.2)	12.2 (12.3)	3.2 (3.2)
$CdCl_2$·1.5hys	25.3 (25.6)	13.5 (15.0)	3.9 (3.9)
$CdCl_2$·cys	11.2 (11.8)	3.7 (4.6)	2.9 (2.6)
$CdCl_2$·1.5cys	14.0 (14.7)	4.9 (5.7)	3.6 (2.9)

The infrared spectra for the free amino acids and the respective adduct are shown in Figs 2 and 3. For histidine, the main infrared bands to be considered are that located at 1639, 1581, 1499, 1415 and 1168 cm^{-1}, attributed to the $\nu_a(COO^-)$, $\delta(NH)_3^+$, ν(ring), $\nu_s(COO^-)$ and $\delta(NH)_{imid.}$, respectively [14]. In both adducts with histidine, the $\nu_a(COO^-)$, $\delta(NH)_3^+$, ν(ring) and $\delta(NH)_{imid.}$ bands are almost in the same positions found for the free amino acid. On the other hand, the $\nu_s(COO^-)$ band is shifted to 1400 cm^{-1} for both adducts. The shift towards lower wavenumbers exhibited by the $\nu_s(COO^-)$ band provided evidence that histidine is bonded to the metal ion through the carboxylic group [6, 11, 15].

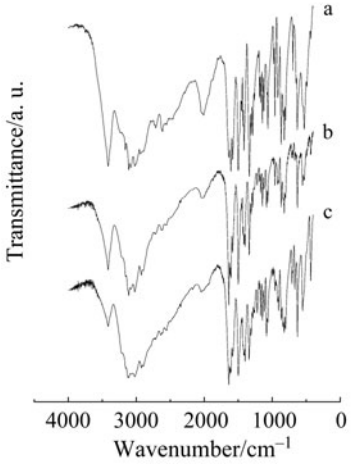

Fig. 2 Infrared spectra for a – histidine; b – $CdCl_2$·1.5his and c – $CdCl_2$·his obtained from powders in KBr discs

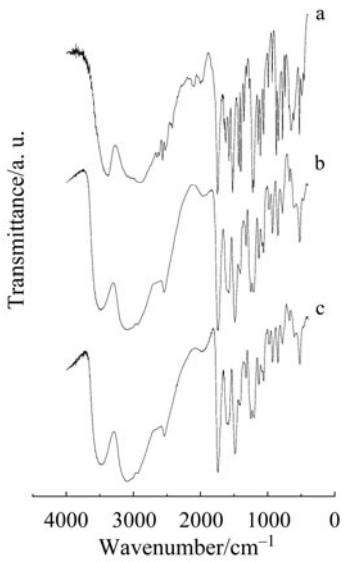

Fig. 3 Infrared spectra for a – cysteine; b – $CdCl_2$·1.5cys and c – $CdCl_2$·cys obtained from powders in KBr discs

For free cysteine, the main infrared bands are located at 1746 cm^{-1} due to ν_aC=O vibration mode. For adducts, ν_aC=O band is shifted to 1736 and 1739 cm^{-1} for $CdCl_2$·cys and $CdCl_2$·1.5cys, respectively, indicating that coordination occurred through the carbonylic oxygen atom [11, 15]. The fact that oxygen and not sulfur is used for coordination seems to be unexpected result when this analysis is based on the hardness of the basic and acidic centers considered.

Thermogravimetric and DSC curves for adducts of histidine and cysteine are shown in Figs 4 to 7, respectively. The adducts $CdCl_2$·cys and $CdCl_2$·1.5cys, Figs 6a and 7a, respectively, started the thermal degradation at 151 and 133°C, exhibiting a calculated mass loss percentage of 46 and 59% respectively, due to the release of ligand molecules. These values are in good agreement with the proposed formula for these adducts. The thermogravimetric data allowed the proposition the following thermal degradation steps for these two adducts: $CdCl_2$·*n*cys (*s*)→$CdCl_2$ (*s*)+*n*cys (*g*), with *n*=1.0 or 1.5, indicating that, as previously noticed for cadmium adducts [16], the rate determining factor in the thermal degradation is the rupture of the metal–ligand bonds. For the histidine adducts, Figs 4a and 5a, respectively, similar sequence of steps of decomposition can be proposed.

The DSC curves for all the synthesized adducts, Figs 4b to 7b, exhibited endothermic peaks in the same temperature range observed for the mass loss steps. On the other hand, the cysteine adducts exhibited an exothermic peak before the endothermic one due to the release of amino acid molecules. This exothermic peak could tentatively be attributed to some kind of structural modification that occurred on the adducts and gave the values of 17 and 19 kJ mol^{-1} for the 1.0 and 1.5 adducts, respec-

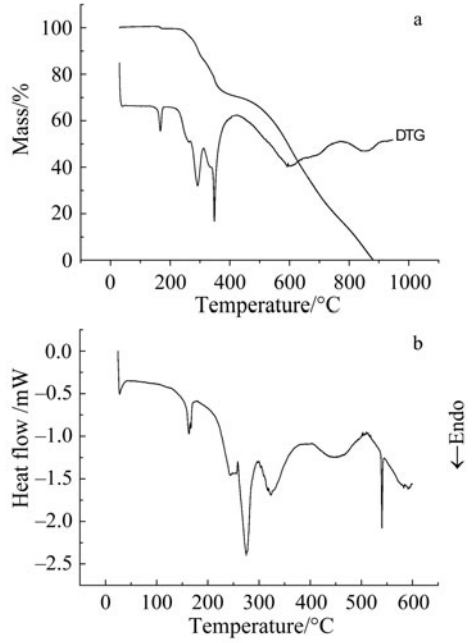

Fig. 4 a – TG and b – DSC curves for the adduct $CdCl_2$·his obtained under argon atmosphere

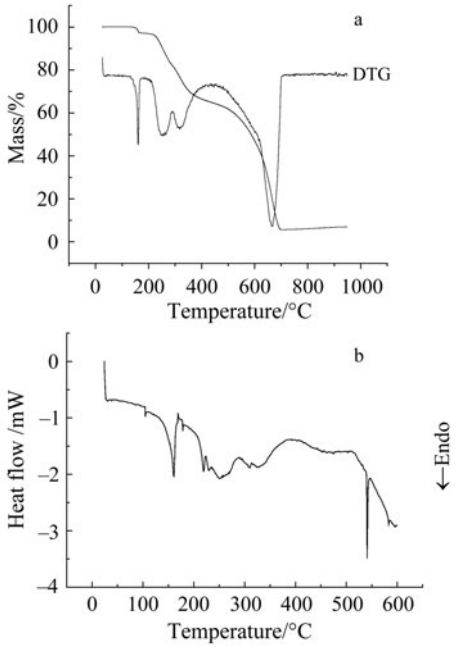

Fig. 5 a – TG and b – DSC curves for the adduct $CdCl_2$·1.5his obtained under argon atmosphere

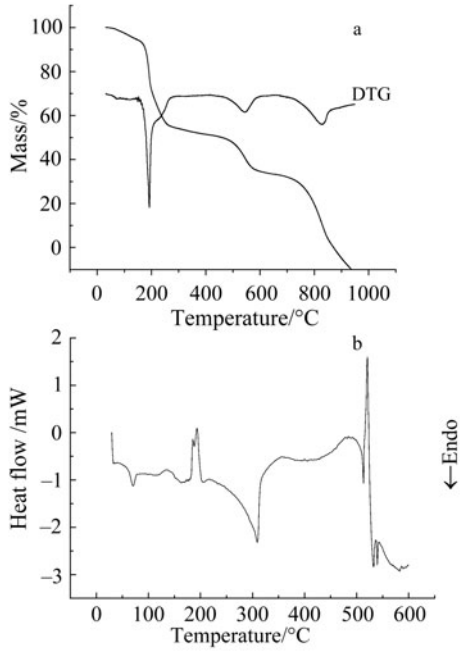

Fig. 6 a – TG and b – DSC curves for the adduct $CdCl_2$·cys obtained under argon atmosphere

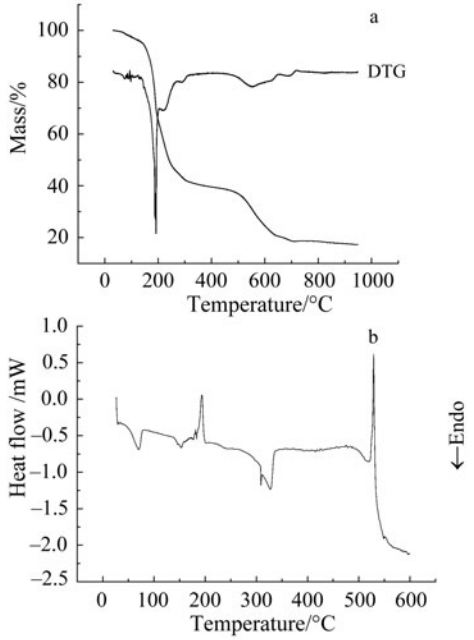

Fig. 7 a – TG and b – DSC curves for the adduct $CdCl_2$·1.5 cys obtained under argon atmosphere

tively. Furthermore, the enthalpic values associated with the release of ligand molecules for the same sequence of adducts are 187 and 102 kJ mol^{-1}, respectively.

For both adducts of histidine, whose DSC curves are shown in Figs 4a and 5a, the last sharp endothermic peak observed in the DSC curve at 540°C is due to the melting of the halide, after the release of the amino acid molecules. The DSC curves for cysteine adducts are shown in Figs 6b and 7b. Both curves are very similar in behavior. The endothermic peak due to the cadmium halide fusion is followed by a deviation of the base line as a consequence of the evaporation, which cause the appearance of a false exothermic peak. For $CdCl_2$·his the mass loss step due to the release of amino acid molecules occurred in the 250–400°C range. The associated endothermic peak corresponded to 35 kJ mol^{-1}. For $CdCl_2$·1.5his the ligands are lost in the same previously presented temperature range to give an enthalpic calculated value of 879 kJ mol^{-1}. Thus, the significant difference in these enthalpic values could only be explained by supposing some kind of difference in the coordination features of the ligand molecules. However, for 1.5 adduct it could be also expected that a ligand can be established a bridge between two cations.

The calculated non-isothermal kinetic parameters obtained from thermogravimetric data by using the Coats–Redfern method [17] are shown in Table 1. As previously reported [18], the non-isothermal Coats–Redfern activation energy values are in good agreement with the isothermal ones for cadmium compounds, which can be used with a high degree of confidence.

Table 2 Non-isothermal thermogravimetric kinetic parameters calculated by using the Coats–Redfern method. E_a/kJ mol^{-1}, n and A are the activation energy, the order of reaction and the frequency or pre-exponential parameters, respectively. Δt/°C is the interval of temperature considered for calculation, B is the number of data used and r is the coefficient of correlation of the obtained straight line

Adduct	E_a	n	A	Δt	B	r
$CdCl_2$·his	77	1	$1.19 \cdot 10^6$	250–354	138	0.986
$CdCl_2$·1.5his	44	1	$1.29 \cdot 10^3$	250–350	107	0.994
$CdCl_2$·cys	55	1	$1.94 \cdot 10^5$	180–266	108	0.952
$CdCl_2$·1.5cys	41	1	$4.38 \cdot 10^3$	175–270	137	0.955

For histidine and cysteine adducts, the activation energy associated with the release of molecules of ligand are larger for mono adducts as presented in Table 2. As previously noticed [16] larger activation energy values for the thermal degradation are related to larger metal–ligand bond enthalpic values. From these data, can be inferred that, the mean metal–ligand bond dissociation enthalpy is also larger for $CdCl_2$·his than for $CdCl_2$·cys. However, for both adducts the metal–ligand bond occurred through the carbonylic oxygen atoms. In conclusion, this fact reflects the great effect caused by the R group on the amino acid when the interaction with metal occurred.

The authors are indebted to CAPES-PICDT (RFF and LMN) and CNPq (CA) for fellowships. FAPESP is also knowledged for financial support.

References

1 R. H. Garret and C. M. Grisham, Biochemistry, Saunders, New York 1995, p. 55.
2 J. J. R. F. da Silva and R. J. P. Williams, The Biological Chemistry of the Elements, Oxford University Press, London 1991.
3 G. L. Patrick, An Introduction to Medicinal Chemistry, Oxford University Press, London 1995.
4 W. Bae and R. K. Mehra, J. Inorg. Biochem., 70 (1998) 125.
5 I. Nemec, I. Císarová and Z. Micka, J. Solid State Chem., 140 (1998) 71.
6 V. Magafa, S. P. Perlepes and G. Stavropoulos, Transition Met. Chem., 23 (1998) 105.
7 E. Kiss, A. Lakatos, I. Bányai and T. Kiss, J. Inorg. Biochem., 69 (1998) 145.
8 N. Nagao, T. Kobayashi, T. Takayama, Y. Koike, Y. Ono, T. Watanabe, T. Mikami, M. Suzuki, T. Matumoto and M. Watabe, Inorg. Chem., 36 (1997) 4195.
9 V. Magafa, G. Stavropoulos, P. Tsiveriotis and N. Hadjiliadis, Inorg. Chim. Acta, 272 (1998) 7.
10 F. Rodante, Thermochim. Acta, 200 (1992) 47.
11 R. F. De Farias, H. Scatena Jr. and C. Airoldi, J. Inorg. Biochem., 73 (1999) 253.
12 R. F. De Farias and C. Airoldi, J. Inorg. Biochem., 76 (1999) 273.
13 A. W. Coats and J. P. Redfern, Nature, 201 (1964) 68.
14 P. A. M. Williams and E. J. Baran, Transition Met. Chem., 22 (1997) 589.
15 R. F. De Farias, O. A. De Oliveira, J. V. De Medeiros and C. Airoldi, Thermochim. Acta, 328 (1999) 241.
16 R. F. De Farias, O. A. De Oliveira, H. Scatena Jr., F. M. Borges, M. De Silva and A. O. Da, Quím., Nova, 21 (1998) 164.
17 A. W. Coats and J. P. Redfern, Nature, 201 (1964) 68.
18 M. C. N. Machado, L. M. Nunes, C. D. Pinheiro, J. C. Machado and A. G. De Souza, Thermochim. Acta, 328 (1999) 201.